

# Application of anisotropic Hyperelastic constitutive model in finite element analysis of flexible deformable bump

†Ying.Xiang<sup>1</sup>, \*Haitao Cui<sup>1</sup> and Hongjian Zhang<sup>1</sup>

<sup>1</sup> Jiangsu Province Key Laboratory of Aerospace Power System, Nanjing 210016, P.R. China  
State Key Laboratory of Mechanics and Control of Mechanical Structures, Nanjing 210016, P.R. China  
Nanjing University of Aeronautics and Astronautics, Nanjing 210016, P.R. China

\*Presenting author:15705186098@163.com

†Corresponding author:1455466692@qq.com

## Abstract

The three-dimensional nonlinear bump model is established by using ABAQUS software. The anisotropic hyperelastic model established by the strain energy density function, which is used to simulate the property of cord - rubber composites in the flexible bump. The main direction of the material can simulate the geometrical and material nonlinearity of the cord - rubber composite. By modeling the bump structure as a whole, the model is simplified and the calculation efficiency and calculation accuracy are improved. The deformation height and inner stress of the bump structure under different inflation pressures are obtained by three-dimensional nonlinear analysis, the large deformation of cord - rubber composite is also taken into account in the analysis.

**Keywords:** bump; anisotropic hyperelastic; cord - rubber composites; nonlinear analysis; deformation

## Introduction

The cord - rubber composite is a flexible composite material formed by the effective combination of the cord and the rubber. It is widely used in tires, inflatable springs, air bags and conveyors. The rubber is a material with a low elastic modulus and a high elongation, while the cord is a material with a high modulus of elasticity and a low elongation. The composite exhibits a high toughness and a high strength by the cooperation of the substrate and the fibers high strength characteristics. Because of the obvious anisotropy and nonlinearity of the cord rubber material during the bearing, the anisotropic hyperelastic constitutive model[1]-[4] can well characterize the characteristics of the cord - rubber composite, and has good engineering practicability.

In this paper, ABAQUS is used to establish the finite element model of the bump. By the UANISOHYPER\_INV interface in the ABAQUS do secondary development of the constitutive model, called the written UANISOHYPER\_INV subroutine as cord - rubber composite constitutive equations during the finite element calculation. This can more accurately simulate the deformation behavior of the cord - rubber composite structure.

### 1. Anisotropic hyperelastic constitutive model

Anisotropic elastic constitutive model is based on the continuum mechanics of fiber reinforced composite material[5]-[7]. the fiber composite material having a direction, the strain energy function can be expressed as the function of the right Cauchy-Green deformation tensor  $\mathbf{C} = \mathbf{F}^T \mathbf{F}$  and the invariant  $I_i$  which is related to the original fiber directional vector  $\mathbf{a}_0$ . Generally have the following form, Here  $\mathbf{F}$  is the deformation gradient tensor

$$W(\mathbf{C}, \mathbf{a}_0) = W_{iso}(I_1, I_2, I_3) + W_{triso}(I_4) \quad 1-1$$

Where  $W_{iso}$  is the isotropic hyperelasticity of the the rubber,  $W_{triso}$  is the anisotropic strain energy due to the reinforcement of the cord; the strain tensor invariant  $I_1, I_2, I_3$  characterizes

the isotropic property of the material, which  $I_4$  is related to the direction of the material.

Where the invariants are given by

$$\begin{aligned} I_1 &= \text{tr}(\mathbf{C}); \quad I_2 = \frac{1}{2}[(\text{tr}\mathbf{C})^2 - \text{tr}(\mathbf{C}^2)] \\ I_3 &= \det(\mathbf{C}); \quad I_4 = \mathbf{a}_0 \cdot \mathbf{C} \cdot \mathbf{a}_0 \end{aligned} \quad 1-2$$

Where  $\mathbf{c} = \begin{bmatrix} \lambda_1^2 & 0 & 0 \\ 0 & \lambda_2^2 & 0 \\ 0 & 0 & \lambda_3^2 \end{bmatrix}$ ,  $\lambda_i$  represents a ratio of three principal directions of elongation material ( $\lambda_i = 1 + \varepsilon_i$ ,  $\varepsilon_i$  represents the strain of principal directions).

In an ideal conditions, the rubber can be regarded as incompressible material, The energy  $W_{iso}$  stored in the matrix is given by the Mooney-Rivlin model[8]-[10] form

$$W_{iso} = \sum_{\substack{ij=n \\ ij=0}} c_{ij} (I_1 - 3)^i (I_2 - 3)^j$$

The Mooney-Rivlin two-parameter strain energy function, which is widely used in ABAQUS finite element software, can be obtained by the first two terms of the equation in the case of sufficiently small deformation

$$W_{iso} = C_{10}(I_1 - 3) + C_{01}(I_2 - 3)$$

Where  $C_{10}$ 、 $C_{01}$  are the material parameters, the unit is Mpa .

The strain energy of the cord is generally considered to be related to the elongation of the cord and equal to the square of the cord draw ratio. Therefore, a polynomial is defined to represent the strain energy of the cord. When the cord is compressed, Can be ignored. The strain energy function of the cord is as follows

$$W_{triso} = \begin{cases} k_1(I_4 - 1)^2 + k_2(I_4 - 1)^3 + k_3(I_4 - 1)^4, & I_4 > 1 \\ 0 \end{cases}$$

Where  $k_1$ 、 $k_2$ 、 $k_3$  are material parameters, in units of Mpa .

In order to obtain a stress-strain constitutive relation of the form, according to the formula 1-1 derived composite material the second Piola- Kirchhoff stress tensor  $\mathbf{S}$  is

$$\mathbf{S} = 2 \frac{\partial W(\mathbf{C}, \mathbf{a}_0)}{\partial \mathbf{C}} = 2 \sum_{m=1}^4 \frac{\partial W(\mathbf{C}, \mathbf{a}_0)}{\partial I_m} \frac{\partial I_m}{\partial \mathbf{C}}$$

Where the invariant  $I_m$  pairs of right Cauchy - Green deformation tensor partial derivatives are as follows:

$$\begin{aligned} \frac{\partial I_1}{\partial \mathbf{C}} &= \mathbf{I} & \frac{\partial I_2}{\partial \mathbf{C}} &= I_1 \mathbf{I} - \mathbf{C} \\ \frac{\partial I_3}{\partial \mathbf{C}} &= I_2 \mathbf{I} - I_1 \mathbf{C} + \mathbf{C}^2 & \frac{\partial I_4}{\partial \mathbf{C}} &= \mathbf{a}_0 \otimes \mathbf{a}_0 \end{aligned}$$

Cauchy stress tensor

$$\boldsymbol{\sigma} = J^{-1} \mathbf{F} \mathbf{S} \mathbf{F}^T = \frac{2}{J} \left[ (W_1 + W_2 I_1 + W_3 I_2) \mathbf{B} - (W_2 + W_3 I_1) \mathbf{B}^2 + W_3 \mathbf{B}^3 + I_4 W_4 \mathbf{a} \otimes \mathbf{a} \right]$$

Which  $W_i$  represents the partial derivative of the invariant,  $\mathbf{B}$  represents the left Cauchy-Green deformation tensor, and the post-deformation cord direction  $\mathbf{a} = \frac{1}{\lambda_F} \mathbf{F} \mathbf{a}_0$ , ( $\lambda_F$  representing the elongation ratio of the cord)

$$\begin{cases} \sigma_1 = 2 \left[ (W_1 + W_2 I_1) \lambda_1^2 - W_2 \lambda_1^4 + W_4 \lambda_1^2 \cos^2 \alpha \right] \\ \sigma_2 = 2 \left[ (W_1 + W_2 I_1) \lambda_2^2 - W_2 \lambda_2^4 + W_4 \lambda_2^2 \sin^2 \alpha \right] \\ \sigma_3 = 2 \left[ (W_1 + W_2 I_1) \lambda_3^2 - W_2 \lambda_3^4 \right] \end{cases}$$

The material parameters in the constitutive model can be fitted by uniaxial tensile experiments  
 (1) Get the rubber matrix material parameters  $C_{10}$  and  $C_{01}$  according rubber uniaxial stretching test data

(2) Get the cord material parameters  $k_1$ ,  $k_2$  and  $k_3$  according uniaxially stretched in the direction of the cord fitting experimental data

The tensile test data is fitted by the least squares method to obtain the material parameters in the constitutive model as shown in the following table

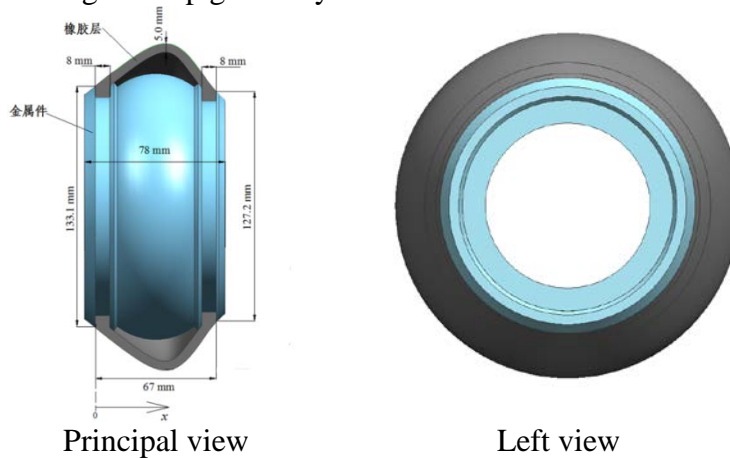
**Table 1. Material parameters**

$C_{10}$	$C_{01}$	$k_1$	$k_2$	$k_3$
-0.89	1.78	13.43	-17.88	14.45

## 2. Three-dimensional finite element model of bump

### 2.1 Three-dimensional structure of the bump

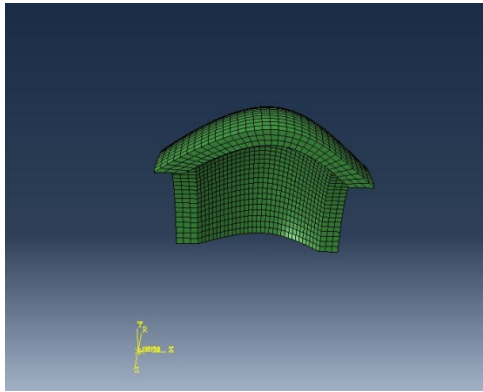
The actual geometry of bump is complicated, get the airbag outside the cavity when set up the finite element model, as show in the figure(a) . the airbag on both sides of the metal chamber is determined by applying a fixed boundary conditions . the airbag section around the central axis of rotation to get bump geometry model.



Figure(a)

### 2.2 Mesh and element type

The bump structure is divided into three-layer. And the bump are constructed by different material layers. The unit of the model is C3D8 , a total of 3840 units 6412 nodes, as show in the figure(b).



Figure(b)

### 2.3 Grid division and cell type

Due to the use of cord - rubber composites in the drum structure, the drum structure is divided into three-layer units when the meshes are divided, and the drums are constructed by different material layers. Three-dimensional model using 8- node entity unit, a total of 3840 units 6412 nodes.

### 2.4 Material model

The rubber layer use the Mooney-Rivlin material model, cord - rubber composite material layer using an anisotropic elastic constitutive material models, When defining the cord - rubber composite layer, the direction of the material can be assigned according to the actual laying angle of the cord.

### 2.5 Boundary conditions and load conditions

Considered the bump and the metal cavity fixed constraint , set the completely fixed constraint of two sides of bump, regard the inflation pressure as a uniform load for the inner surface of the bump in the simulation analysis.

## 3. Calculation result and analysis

Table 2 is the maximum deformation height of bump structure under the different loads and different cord angle, figure (c) is a maximum deformation height of bump structure under different load and the same cord angle; figure(d) is the maximum deformation height of bump structure under different cord angle and the same load.

**Table 2. the maximum deformation height of bump**

load/Pa angle	0.1	0.3	0.5	0.7	0.9
15°	83.09	84.42	85.78	87.18	88.60
30°	83.21	84.77	86.36	88.01	89.70
45°	83.43	85.38	87.40	89.55	91.77
60°	83.72	86.19	88.82	91.78	94.72

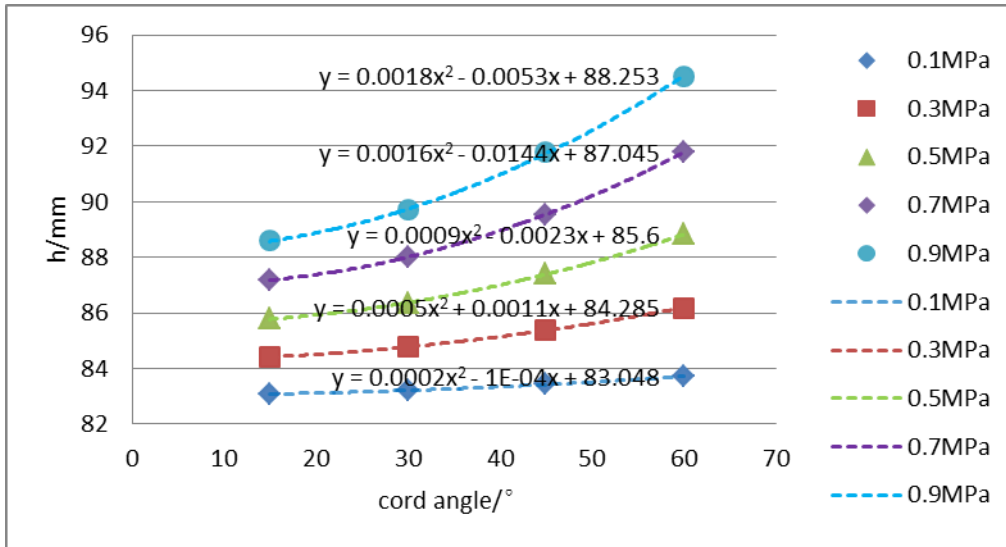


Figure (c)

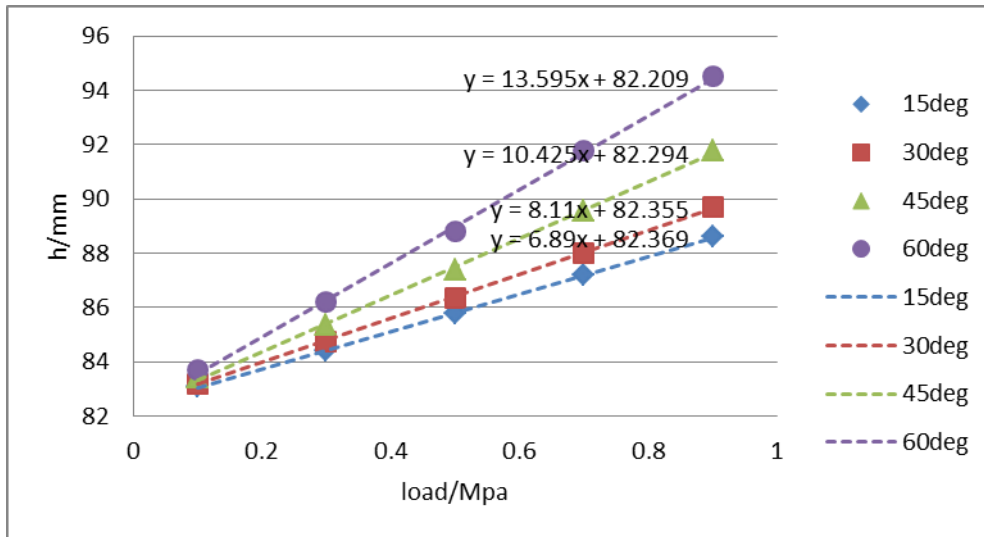


Figure (d)

It can be seen from figure(c) that the maximum deformation height of the bump increases by the increase of the uniform load in the bump inner surface at the same cord angle, and the maximum deformation height of the bump under different loads is approximately in a straight line , It can be shown that the maximum deformation height of the bump increases linearly with the increase of the uniform load when the cord angle is unchanged. As can be seen from figure(d) , with the uniform distribution load, The maximum deformation height of the bump is also increased by the increase of the cord angle, the maximum deformation height of the bump is approximately in a quadratic curve. In figure(c) and figure(d) , the curve function expression acquired by the least squares method fit.

#### 4.Conclusions

The cord-rubber composite material is a nonlinear material. The anisotropic hyperelastic constitutive model can simulate the deformation behavior of the cord-rubber accurately, and provide the analytical basis for the design and optimization of the bump structure in the subsequent finite element analysis.

## References

- [1] Peng XQ, Guo ZY and Moran B. An anisotropic hyperelastic constitutive model with fiber-matrix shear interaction for the human annulus fibrosus. *Journal of Applied Mechanics*, 2006, 73: 815-824.
- [2] Guo Guodong, Peng Xiongqi and Zhao Ning. An anisotropic hyperelastic constitutive model with shear interaction for cord-rubber tire composites. *Chinese Journal of Theoretical and Applied Mechanics*, 2013, 45(3):451-455.
- [3] Sun Shulei, Mao Jianliang and Peng Xiongqi. An Anisotropic Hyperelastic Constitutive Model With Fibre Bending Stiffness for Cord-Rubber Composites. *Applied Mathematics and Mechanics*, 2014, 35(5):471-477.
- [4] Huang Xiaoshuang, Peng Xiongqi and Zhang Bichao. An anisotropic visco-hyperelastic constitutive model for cord-rubber composites. *Chinese Journal of Theoretical and Applied Mechanics*, 2016, 48(1):140-145.
- [5] Spencer A J M. *Continuum Theory of the Mechanics of Fibre-Reinforced Composites*. *Journal of Applied Mechanics*, 1984, 53(1):233.
- [6] Clark SK. Theory of the elastic net applied to cord-rubber composites. *Rubber Chemistry and Technology*, 1983, 56(2): 372-389.
- [7] Ishikawa S, Tokuda A, Kotera H. Numerical simulation for fibre reinforced rubber. *Journal of Computational Science and Technology*, 2008, 2(4): 587-596.
- [8] L. R. G. Treloar. The elasticity of a network of long-chain molecules I/II. *Trans Faraday Soc*, 1943, 42(4):83-94.
- [9] Boyce M C, Arruda E M. Constitutive Models of Rubber Elasticity: A Review[J]. *Rubber Chemistry & Technology*, 2000, 73(3):504-523.
- [10] Rivlin R S. Large Elastic Deformations of Isotropic Materials. V. The Problem of Flexure[J]. *Proceedings of the Royal Society A*, 1949, 195(1043):463-473.